



Research paper

Characterization and pharmacokinetic analysis of aerosolized aqueous voriconazole solution

Justin A. Tolman^a, Nicole A. Nelson^a, Yoen Ju Son^a, Stephanie Bosselmann^a, Nathan P. Wiederhold^{a,b}, Jay I. Peters^c, Jason T. McConville^a, Robert O. Williams III^{a,*}^a College of Pharmacy, The University of Texas at Austin, TX, USA^b Pharmacotherapy Education and Research Center, The University of Texas Health Science Center at San Antonio, TX, USA^c Department of Medicine, University of Texas Health Science Center at San Antonio, TX, USA

ARTICLE INFO

Article history:

Received 6 October 2008

Accepted in revised form 18 December 2008

Available online 14 January 2009

Keywords:

Voriconazole
Antifungal
Cyclodextrin
Pharmacokinetics
Single dose
Multiple dose
Inhaled
Pulmonary
Mouse
Animal
Isotonic

ABSTRACT

Invasive fungal infections in immunocompromised patients have high mortality rates despite current treatment modalities. This study was designed to evaluate the suitability of an aqueous solution of voriconazole solubilized with sulfobutyl ether- β -cyclodextrin for targeted drug delivery to the lungs via nebulization. A solution was prepared such that the inspired aerosol dose was isotonic with an acceptable mass median aerodynamic diameter of 2.98 μm and a fine particle fraction of 71.7%. Following single and multiple inhaled doses, high voriconazole concentrations were observed within 30 min in the lung tissue and plasma. Drug solubilization with sulfobutyl ether- β -cyclodextrin contributed to the rapid and high drug concentrations in plasma following inhalation. Maximal concentrations in the lung and plasma were $11.0 \pm 1.6 \mu\text{g/g}$ wet lung weight and $7.9 \pm 0.68 \mu\text{g/mL}$, respectively, following a single inhaled dose with a corresponding tissue/plasma concentration ratio of 1.4 to 1. Following multiple inhaled doses, peak concentrations in lung tissue and plasma were $6.73 \pm 3.64 \mu\text{g/g}$ wet lung weight and $2.32 \pm 1.52 \mu\text{g/mL}$, respectively. AUC values in lung tissue and plasma were also high. The clinically relevant observed pharmacokinetic parameters of inhaled aqueous solutions of voriconazole suggest that therapeutic outcomes could be benefitted through the use of inhaled voriconazole.

© 2009 Elsevier B.V. All rights reserved.

1. Introduction

Invasive fungal infections are increasing in prevalence in immunocompromised patients due to decreased immunity resulting from drug therapy, organ transplantation, and/or various disease states [1]. The distribution of causative organisms for invasive fungal infections has been changing with an increase in the prevalence of *Aspergillus* spp. and other invasive molds [2]. Systemic fungal infections caused by *Aspergillus* spp. are primarily lung infections due to the inhalation of conidia. The resulting infection, Invasive Aspergillosis (IA), is the cause of serious damage to lung tissue due to invasive hyphal growth [3]. Dissemination of IA can also occur to other organ systems, and correlates with a poorer prognosis [4]. Despite the best therapeutic options, mortality rates for IA remain high [4,5].

The primary therapy for the treatment of IA is the systemic administration of voriconazole, and has led to improved patient outcomes compared to other treatments [6,7]. Voriconazole is a tri-

azole antifungal with broad antifungal activity against numerous pathogenic fungi in addition to its activity against *Aspergillus* spp. [8,9]. Voriconazole has also been reported to distribute to the lungs as measured by tissue and epithelial lining fluid concentrations following systemic administration [10,11]. The commercial voriconazole product, Vfend®, is available as an oral tablet or intravenous formulation. The intravenous product is formulated with Captisol®, sulfobutyl ether- β -cyclodextrin, to form a solubilized drug-cyclodextrin complex due to very slight voriconazole solubility in water [12]. Voriconazole has reported side effects of visual disturbances, hepatic toxicity, and dermatologic reactions as well as serious cytochrome P450 mediated drug interactions [8,10]. Adverse events causing discontinuation of therapy occurred in up to 6% of patients, and were primarily due to elevations in liver function tests or rash. Other systemically administered antifungals can be selected as salvage therapy or in patients intolerant to voriconazole, but have the potential for other serious side effects as well as drug interactions [6,13,14].

The potential side effect profile and drug interactions associated with systemic antifungal administration might be reduced by targeting drug delivery to the lungs, the primary site of IA. Targeted lung delivery of antifungals can also lead to high drug

* Corresponding author. The University of Texas at Austin, College of Pharmacy, 1 University Station, A1900, Austin, TX 78712, USA. Tel.: +1 512 471 4681.

E-mail address: williro@mail.utexas.edu (R.O. Williams).

concentrations at the site of infection to improve clinical outcomes. Two antifungals, amphotericin B and itraconazole, have been inhaled with the reported pharmacokinetic and outcome measures [13,15–23]. Inhaled amphotericin B formulations include drug solubilized with deoxycholate, drug encapsulated in liposomes, and drug–lipid complexed suspensions. Inhaled itraconazole was formulated as crystalline or amorphous nano-particulate suspensions.

Inhaled amphotericin B has a better but non-optimal side effect profile and significantly improved outcomes compared to the systemically administered formulations [13,15,17,23]. However, the pharmacokinetic profiles of inhaled compared to intravenous amphotericin B are substantially different. Lung concentrations of amphotericin B following intravenous administration are initially undetectable followed by low levels despite extensive tissue distribution following multiple doses [24–28]. Inhaled amphotericin B has led to much higher lung tissue concentrations but undetectable plasma levels [16,29,30]. The high drug concentrations in the lung tissue following amphotericin B inhalation was hypothesized to result in significant outcomes in human patients and animal models of IA compared to intravenous drug administration [15,17].

Inhaled nano-particulate itraconazole was also well tolerated with normal histological findings and an absence of inflammatory mediators following a chronic, multi-dose study in animals [22]. The pharmacokinetic profile of different inhaled formulations following a single inhaled dose demonstrated high and prolonged itraconazole concentrations in the lungs with maximal lung levels achieved 30–60 min after the completion of nebulization, while serum concentrations remained low and peaked after 2–5.35 h in animals [20,21,31]. The ratio of lung-to-serum AUC values was 25–50 and C_{\max} ratios ranged from approximately 10 to 100, indicating low drug partitioning out of the lungs. Following multiple doses, lung concentrations remained substantially higher than serum concentrations [21]. Inhaled itraconazole demonstrated significantly improved outcomes compared to oral itraconazole and control groups in animal models of IA, and was suggested to be due to sufficient drug concentrations in the lungs to inhibit invasive fungal growth at a fraction of the oral dose [18,19].

Both inhaled amphotericin B and inhaled particulate itraconazole demonstrated substantial drug retention in the lungs, improved survival in the animal models of IA, and suggested positive clinical outcomes were associated with favorable lung pharmacokinetic profiles. Gavalda and colleagues reported an improved survival in an animal model of IA when both inhaled and intravenous antifungal were administered concurrently compared to inhaled or intravenous drug administered separately [15]. This report suggests near-therapeutic plasma concentrations combined with very high concentrations of antifungal in the lung could improve patient outcomes. However, neither inhaled amphotericin B nor inhaled itraconazole produces blood concentrations that are close to therapeutic levels. Therefore, targeted delivery of an antifungal to the lungs with distribution to the blood producing high drug concentrations in both lung tissue and blood can potentially improve clinical outcomes and be a significant improvement in antifungal therapeutic options.

The poor distribution of amphotericin B and itraconazole to the systemic circulation following inhalation could be due, in part, to the very low aqueous solubilities of these compounds. Inhalation of a solubilized antifungal, the voriconazole–cyclodextrin inclusion complex as Vfend® IV, could lead to better lung concentrations than reported following systemic drug administration as well as systemic drug distribution. In this study, it is hypothesized that an aqueous solution of voriconazole solubilized with sulfobutyl ether- β -cyclodextrin, when inhaled as a single dose, would produce high lung drug concentrations as well as allow rapid distribution from the lungs to the plasma. Furthermore, following multiple doses, inhaled voriconazole solutions would also produce elevated

and consistent trough concentrations in lungs and plasma. Although solubilized voriconazole should distribute to the systemic circulation following inhalation, reductions in the incidence of hepatotoxicity, visual abnormalities, and dermatologic reactions could still occur due to a lower drug burden and dose sparing compared to systemic drug administration.

2. Materials and methods

2.1. Materials

Vfend® IV (Pfizer Inc., New York, NY, USA), voriconazole, and sulfobutyl ether- β -cyclodextrin, Captisol® were generously supplied by CyDex Pharmaceuticals, Inc. (Lenexa, KS). Sterile water for injection (SWFI) (Hospira, Inc.) and normal saline were purchased from Cardinal Health (Dublin, OH). Sodium tetraborate decahydrate, boric acid, and sodium acetate trihydrate were purchased from Sigma–Aldrich, Inc. (St. Louis, MO). Acetic acid was purchased from Sigma–Aldrich Laborchemikalien GmbH (Seelze, Germany). HPLC grade ethyl acetate was purchased from Spectrum Chemical Manuf. Corp. (Gardena, CA). HPLC grade acetonitrile was purchased from Fisher Scientific (Fair Lawn, NJ). HPLC grade methanol was purchased from EMD Chemicals Inc. (Gibbstown, NJ). Water was obtained from an in-house Milli-Q UV Plus water purification system from the Millipore Corp. (Billerica, MA).

2.2. Characterization of *in vitro* properties of voriconazole solutions

Vfend® IV was reconstituted with SWFI as instructed in the prescribing information to a 10 mg/mL voriconazole concentration, which also contained sulfobutyl ether- β -cyclodextrin at 160 mg/mL. Additional dilutions were prepared with SWFI to voriconazole concentrations from 2.5 mg/mL to 10 mg/mL. The osmolality of voriconazole solutions was tested ($n = 10$ per concentration) using a μ Osmette Micro Osmometer (Precision Systems Inc., Natick, MA). The pH of the 6.25 mg/mL voriconazole dilution was determined using an Orion 350 PerpHecT® Advanced Benchtop pH Meter (Thermo Fisher Scientific, Waltham, MA).

2.3. Particle size analysis using a cascade impactor

Voriconazole solutions were diluted to 6.25 mg/mL voriconazole and aerosolized using an Aeroneb® Pro micro pump nebulizer (Nektar Therapeutics, San Carlos, CA) for 20 min. Aerodynamic droplet size distributions were determined using a USP Apparatus 1 non-viable eight-stage cascade impactor (Thermo-Anderson, Smyrna, GA) to quantify total emitted dose (TED) from the nebulizer output, mass median aerodynamic diameter (MMAD), geometric standard deviation (GSD), and percentage droplets with an aerodynamic diameter less than 4.7 μ m (defined as the percentage fine particle fraction or FPF). The characterization of aerodynamic droplet size distribution was conducted through modifications to the guidelines described in USP 30 Section 601: Aerosols, Nasal Sprays, Metered-dose Inhalers, and Dry Powder Inhalers [32].

2.4. Single-dose pharmacokinetic analysis

Male outbred ICR (Institute for Cancer Research) mice were purchased from Harlan Sprague Dawley, Inc. (Indianapolis, IN) and housed with free access to water and food. Prior to dosing, mice were acclimated to the nose-only dosing animal restraints. Mice received a single inhaled dose of 5 mL aqueous voriconazole solution at 6.25 mg/mL voriconazole using a nose-only dosing apparatus with a drug exposure time of 20 min. Single-dose pharmacokinetic profiles were determined in two groups of mice:

a high flow-rate group (5 L/min air flow, 32 g average mouse mass) and low flow-rate group (1 L/min, 22 g average mouse mass). Two or more mice were euthanized by carbon dioxide narcosis at each time point (high flow-rate: 5, 10, 20, 30, 60, 90, 150, 240, 360, 720, and 1440 min or low flow-rate mice: 10, 30, 60, 240, 360, and 480 min). Whole blood was collected by cardiac puncture into heparinized vials and centrifuged at 9000RPM for 15 min to obtain plasma. Whole lungs were also collected following exsanguination. Plasma samples and whole lungs were frozen and stored at -20°C until assayed. Lungs were thawed and homogenized with 1 mL of water using an Omni GLH homogenizer (Omni International, Marietta, GA). Plasma samples and lung homogenates were analyzed individually for each animal sampled for voriconazole concentration by reverse-phase high-performance liquid chromatography (HPLC). Concentration values were then averaged and used to determine the concentration versus time profiles. All animals were handled and maintained in accordance with The University of Texas at Austin Institution Animal Care and Use Committee (IACUC) guidelines and in accordance with the American Association for Accreditation of Laboratory Animal Care guidelines.

2.5. Multi-dose pharmacokinetic analysis

Male ICR mice weighing, on average, 22.5 g, were administered inhaled voriconazole twice daily using a nose-only dosing apparatus as described above. Doses were administered for 12 consecutive days beginning each day at 08:00 and 16:00. Airflow through the dosing apparatus was constant at 1 L/min throughout the study. The dosing apparatus was disassembled and cleaned between each use. Randomly selected groups of 6 mice were sacrificed by carbon dioxide narcosis on days 3, 5, 10, and 12. For trough concentration determination, lung and plasma samples were collected immediately before the next scheduled morning dose on days 3, 5, 10, and 12 (16 h after the last dose). For the determination of peak voriconazole concentrations (C_{max}), lung and plasma samples were collected 30 min after the completion of the 10th dose on day 5 of administration. Lung and plasma samples were handled and processed as described in the single-dose methodological description.

2.6. Chromatographic analysis

Calibration standards, plasma, and homogenized lung samples were analyzed using similar methods to those previously published [33,34]. Briefly, voriconazole was extracted from plasma samples through the addition of acetonitrile, centrifugation, and supernatant extraction. The supernatant liquid was evaporated under a gentle stream of nitrogen and residual solids, including voriconazole, were re-dispersed with mobile phase and analyzed spectrophotometrically. For lung homogenate, 0.2 M borate buffer (pH 9.0) was added followed by three liquid-phase extractions with ethyl acetate. The liquid from collected supernatant fractions were then evaporated under a gentle stream of nitrogen. Any residual solids, including voriconazole, were re-dispersed with mobile phase, centrifuged, and then analyzed spectrophotometrically. Each voriconazole sample was analyzed using a Waters Breeze liquid chromatograph (Waters Corporation, Milford, MA) or Shimadzu LC-10 liquid chromatograph (Shimadzu Corporation, Columbia, MD) equipped with a heated (35°C) Jupiter[®] C18 (150 mm \times 4.6 mm, 5 μm) with a Universal security guard (Widopore C18) guard column (Phenomenex, Torrance, CA). The sample volume was 50 μL with a UV detection wavelength of 254 nm. The mobile phase consisted of a 50:50 mixture of 0.01 M, pH 5.0, sodium acetate buffer and methanol at 1.0 mL/min.

2.7. Pharmacokinetic analysis

Observed pharmacokinetic parameters were evaluated from the voriconazole concentration versus time profiles in plasma and lung tissue using independent non-compartmental models. The peak concentration (C_{max}) and the time to achieve the C_{max} (T_{max}) were determined. In addition, the area under the curve (AUC) in lung tissue and plasma up to 6 h after the completion of drug exposure was calculated using the trapezoidal rule.

2.8. Statistical analysis

Maximal concentrations in lung tissue and plasma were compared for statistical analysis by the *t*-test. Single dose C_{max} values were compared by a paired *t*-test with a *P*-value of <0.05 for significance. Multiple dose C_{max} values were compared using a *t*-test assuming unequal variance with a *P*-value of <0.05 for significance.

3. Results

3.1. In vitro solution characterization

The osmolality of aqueous solutions of voriconazole and sulfobutyl ether- β -cyclodextrin was correlated with solute concentrations. The osmolality for voriconazole solutions that contained sulfobutyl ether- β -cyclodextrin between 40 and 160 mg/mL was 109.3–507.7 mOsm/kg, respectively. A solution containing 6.25 mg/mL voriconazole and 100 mg/mL sulfobutyl ether- β -cyclodextrin was isotonic with an osmolality of 293.2 mOsm/kg (Fig. 1). The pH of the 6.25 mg/mL voriconazole solution ranged from 6.4 to 6.8.

3.2. Particle size analysis

The aerodynamic particle size distribution of nebulized 6.25 mg/mL voriconazole solution was determined independently in duplicate using an 8-stage non-viable cascade impactor with a spacer and an air-flow rate of 28.3 L/min. Sufficient voriconazole solution was added to the nebulizer medication reservoir such that volume remained after a 20-min nebulization. The average TED, FPF, MMAD, and GSD were 25.51 ± 6.25 mg, $71.7 \pm 2.62\%$, 2.98 ± 0.06 μm , and 2.20 ± 0.13 , respectively.

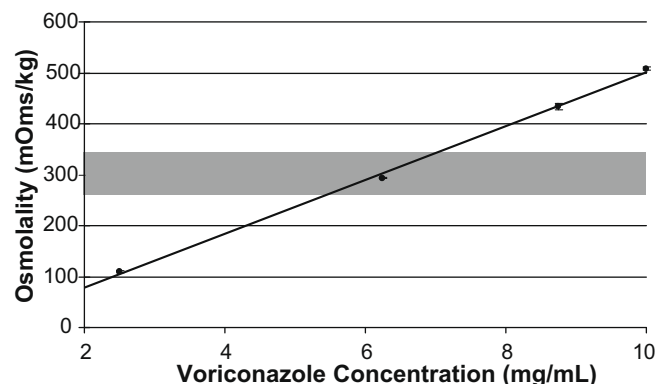


Fig. 1. Osmolality of aqueous solutions in a fixed mass ratio of 1–16 of voriconazole and sulfobutyl ether- β -cyclodextrin. The shaded region indicates the limits of isotonicity. Error bars represent one standard deviation ($N = 10$). The fitted line has a correlation coefficient of 0.998.

3.3. Single-dose pharmacokinetic studies

Following a single inhaled dose of voriconazole, the observed T_{max} values ranged from 10 to 30 min in lung tissue and 20 to 30 min in plasma (Table 1). Voriconazole concentrations in lung tissue were low to undetectable 6–8 h after a single dose while plasma levels remained quantifiable for up to 24 h after the completion of nebulization. In mice that received nebulized voriconazole at an air flow rate of 5 L/min, peak lung concentrations were 1.6 $\mu\text{g/g}$ wet lung weight with an AUC_{0-6} value of 205.3 $\mu\text{g min/g}$ wet lung weight (Fig. 2A). A peak plasma concentration of 1.2 $\mu\text{g/mL}$ and AUC_{0-6} of 136.4 $\mu\text{g min/mL}$ was achieved in this high air flow rate group (Fig. 2B). In contrast, markedly, though not statistically significant ($P > 0.05$), higher peak lung concentration, 11.0 $\mu\text{g/g}$, and AUC_{0-6} , 2408.0 $\mu\text{g min/g}$ were achieved in mice that were exposed to nebulized voriconazole at a slower air flow rate of 1 L/min. Similarly, a higher peak plasma concentration, 7.1 $\mu\text{g/mL}$, and AUC_{0-6} , 1549.8 $\mu\text{g min/mL}$ was also achieved in this low air flow rate group.

3.4. Multiple dose pharmacokinetic studies

In the multiple dose pharmacokinetic study, 5 mL of 6.25 mg/mL voriconazole solution was administered twice daily, beginning at 08:00 and 16:00, for 12 days to mice at the low air flow rate, 1 L/min. Trough lung and plasma samples were taken immediately before the 08:00 dose on days 3, 5, 10, and 12. Peak lung and plasma samples were taken 30 min following the completion of the 08:00 dose on day 5. After 5 days of drug administration, peak voriconazole lung and plasma concentrations were 6.73 $\mu\text{g/g}$ wet lung weight and 2.32 $\mu\text{g/mL}$, respectively. Peak plasma concentrations were significantly lower ($P < 0.05$) following multiple doses than following a single inhaled dose. Peak lung concentrations were not statistically significant for single and multiple doses. Trough lung concentrations of voriconazole were not detectable through day 5 but reached 0.11 to 0.19 $\mu\text{g/g}$ wet lung weight on days 10 and 12, respectively. In contrast, trough plasma voriconazole concentrations were quantifiable on each day of sampling and ranged from 0.18 to 0.32 $\mu\text{g/mL}$ (Table 2).

4. Discussion

The lungs are the primary site of IA due to inhalation of fungal conidia resulting in a focal fungal infection in the lungs that can disseminate to other systems. The site of an IA infection within the lungs is typically in deep alveolar spaces with possible sites of intra-cavity aspergillomas and vascular invasions. Although typical humans are not at risk for IA due to competent immune systems and effective clearance of inhaled spores, immunocompromised patients are at elevated risk for IA and are the focus of prophylactic and treatment regimens with systemic antifungal administration [6,35]. Systemically administered antifungals must distribute to the lungs to be effective therapeutic options but have high reported rates of mortality, in part, due to poor

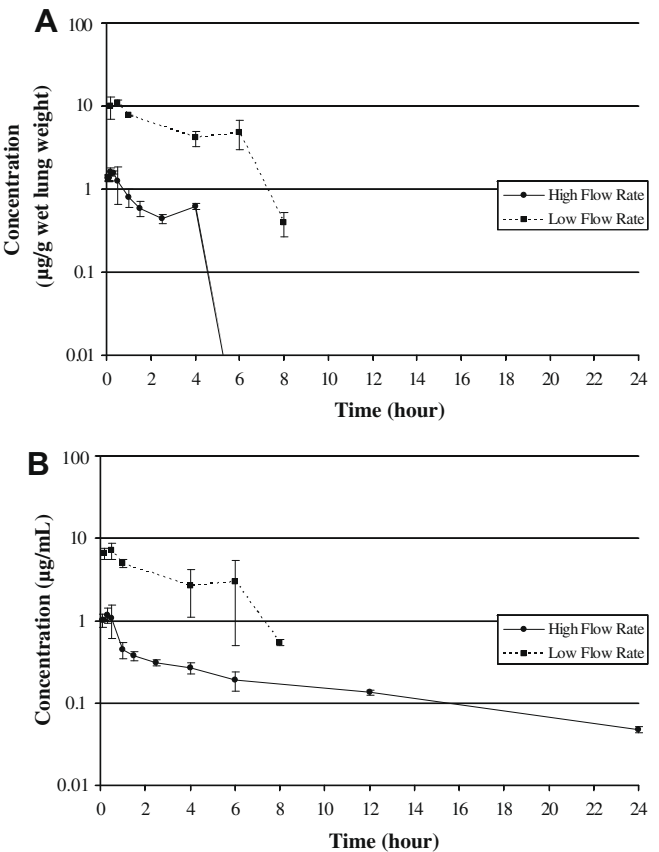


Fig. 2. Pharmacokinetic profile of voriconazole in lung tissue (A) and plasma (B) following a single inhaled dose of aqueous voriconazole solution. The inhaled dose was 5 mL of 6.25 mg/mL voriconazole solution nebulized over 20 min to mice in a nose-only dosing chamber. Errors bars represent one standard deviation ($N = 2$, except $N = 4$ for 1 hour time point for low flow rate group and $N = 1$ for 10-min time point for low-flow rate group). Voriconazole was undetectable in lung tissue 6, 12, and 24 h after the completion of nebulization.

tissue penetration [7,9,10,14,28,36,37]. Targeted antifungal delivery has been reported to cause high drug concentrations at the site of infection in the lung and lead to improved outcomes [20,21,29–31,38]. The studies to date have also demonstrated that targeted antifungal delivery to the lungs has not led to the distribution of drug to the plasma. Interestingly, Gavalda et al., found that a combination of inhaled and intravenous amphotericin B led to improved survival in a rat model of IA. Therefore, having high antifungal concentrations in lung tissue and plasma can potentially lead to improved outcomes in IA. The current study found that an aerosolized aqueous solution of voriconazole solubilized with sulfoethyl ether- β -cyclodextrin was compatible with inhalation and led to high concentrations in the lung tissue as well as plasma following single and multiple doses in a murine pharmacokinetic model of inhalation.

Table 1
Single-dose Pharmacokinetic Parameters for Inhaled Voriconazole. The inhaled dose was 5 mL of 6.25 mg/mL voriconazole solution nebulized over 20 min to mice in a nose-only dosing chamber. All values are the reported average except for the observed T_{max} . The values for C_{max} are the average \pm standard deviation ($N = 2$). The AUC was calculated for concentration versus time profiles from 0 to 6 h by the trapezoidal method.

	Air flow rate (L/min)	Mouse mass (g)	Lung mass (g)	Vfend conc. (mg/mL)	T_{max}		C_{max}		AUC_{0-6}	
					Lung (min)	Plasma (min)	Lung ($\mu\text{g/g}$)	Plasma ($\mu\text{g/mL}$)	Lung ($\mu\text{g min/g}$)	Plasma ($\mu\text{g min/mL}$)
High-flow rate	5.2–5.4	31.8	0.23	6.23	10	20	1.6 \pm 0.17	1.2 \pm 0.25	205.3	136.4
Low-flow rate	1.0	21.8	0.17	6.90	30	30	11.0 \pm 1.6	7.1 \pm 0.68	2408.0	1549.8

Table 2

Multi-dose pharmacokinetic parameters for inhaled voriconazole. Inhaled voriconazole was administered at 08:00 and 16:00 for 12 days. The inhaled dose was 5 mL of 6.25 mg/mL voriconazole solution nebulized over 20 min to mice in a nose-only dosing chamber. Trough values were determined from samples taken immediately before the 08:00 dose while peak samples were taken 30 minutes after the 08:00 dose. Average values are reported \pm standard deviation for $N=6$ mice per value. *Values were below the lower limit of quantitation.

Day	Lung voriconazole concentration ($\mu\text{g/g}$ wet lung weight)		Plasma voriconazole concentration ($\mu\text{g/mL}$)	
	Peak	Trough	Peak	Trough
3	–	*	–	0.22 ± 0.08
5	6.73 ± 3.64	*	2.32 ± 1.52	0.28 ± 0.14
10	–	0.11 ± 0.09	–	0.18 ± 0.09
12	–	0.19 ± 0.23	–	0.32 ± 0.08

Inhaled aerosols must be compatible with biological membranes of the respiratory tract to avoid reactive and inflammatory airway side effects, including cough, dyspnea, and irritation [39,40]. Our results demonstrated that an aqueous solution of voriconazole solubilized with sulfobutyl ether- β -cyclodextrin was compatible with aerosol administration. The 6.25 mg/mL voriconazole dilution had an acceptable pH and was the only tested concentration within the isotonic range (Fig. 1). When this concentration was aerosolized using an Aeroneb[®] Pro vibrating mesh nebulizer system, the *in vitro* aerodynamic particle size characteristics of MMAD and FPF, 2.98 μm and 71.7%, respectively, suggest that the nebulized droplets have a particle size distribution appropriate for inspiration to the deep lung.

Following a single inhaled dose of voriconazole, quantifiable voriconazole concentrations were observed in mice that received low and high doses as determined by the varied air-flow rate from 1 to 5 L/min. At 5 L/min airflow through the dosing chamber, a dilute cloud of voriconazole-containing nebulized droplets was present in the dosing chamber which led to a low dose. Conversely, a more concentrated and stagnant cloud of voriconazole-containing droplets was present at 1 L/min airflow rate through the chamber which led to a higher dose of voriconazole in those mice. This dose difference led to a 7-fold increase in C_{max} values and 11-fold increase in AUC_{0-6} in lung tissue and plasma for mice in the dosing chamber with the slow air flow rate (Table 1). Although peak concentrations and drug exposure were affected by the inhaled dose, voriconazole distribution from the lungs to the plasma was unaffected. Possible drug ingestion due to mucociliary clearance is not a contributing factor to plasma voriconazole concentrations due to hyper-metabolism in mice following oral administration [41]. An approximation of a partition coefficient, based on the lung to plasma ratios of C_{max} and AUC_{0-6} , ranged from 1.4 to 1.6 indicating good absorption and distribution of voriconazole across lung mucosal surfaces. In addition, the observed T_{max} values were observed after 10–30 min in lung tissue and 20–30 min in plasma after the completion of dosing for all mice tested. Additionally, voriconazole concentrations in lung tissue were low to undetectable 6–8 h while plasma levels remained quantifiable for up to 24 h after the completion of nebulization. Therefore, voriconazole was rapidly absorbed and distributed to the central plasma with minimal drug retained in lung tissue.

Inhaled voriconazole achieved maximal concentrations within 30 min in both lung tissue and plasma. The maximal lung tissue concentration was 1.4 times greater than the maximal plasma concentration value. The rapid distribution of voriconazole from lung tissue to plasma as well as the extent of distribution differed substantially from previous reports of inhaled antifungal agents. Specifically, amphotericin B has negligible distribution from lung tissue after inhalation. Following nebulized suspensions of pure amphotericin B, very low serum concentrations were achieved

with a T_{max} of 30 min [29]. Inhaled deoxycholate solutions of amphotericin B produced undetectable plasma concentrations up to 24 h after the dose [27,30]. Additionally, the retention of inhaled amphotericin B in lung tissue has been reported to be 15 to 22 days following a single inhaled dose [38]. For itraconazole, inhaled suspensions of nanoparticulate formulations had lung T_{max} values of 0.5–1 h after the dose but with delayed plasma T_{max} values of 2–5.4 h [20,21,31]. For inhaled itraconazole, the reported AUC values were 25–50 times greater in lung tissue than in the plasma. Similarly, peak itraconazole concentrations were 12–100 greater for lung tissue than plasma. These comparisons indicate negligible distribution of particulate itraconazole from the lungs to the plasma.

The sulfobutyl ether- β -cyclodextrin excipient in inhaled voriconazole solutions prompted the differences in voriconazole distribution compared to inhaled particulate and solubilized amphotericin B as well as inhaled particulate itraconazole. Cyclodextrins have been reported to cause rapid T_{max} and high C_{max} concentrations as well as improved bioavailability of intratracheally administered aerosols or solutions compared to equipotent alternative formulations or routes of administration [42–44]. Although Roffey et al. used a 10 mg/kg IV and 30 mg/kg oral dose, direct comparison to pharmacokinetic parameters observed following a single inhaled dose were not directly possible due to dose uncertainties following inhalation in this study [45]. Additionally, voriconazole displays non-linear pharmacokinetics in humans and animals, which could account for the marked differences observed following inhalation of different doses due to high and low air flow rate through the dosing chamber. However, the observed C_{max} , T_{max} , and AUC values following a single inhaled dose at 1 L/min air flow rate through the dosing chamber were similar to those reported in mice following intravenous drug administration. Therefore, inhaled voriconazole solubilized with sulfobutyl ether- β -cyclodextrin produced plasma pharmacokinetic parameters similar to intravenous drug administration with additional high lung tissue concentrations.

The multi-dose voriconazole pharmacokinetic profile cannot be extrapolated from a single-dose profile due to non-linear pharmacokinetics resulting from saturable hepatic metabolic pathways [8]. Additionally, the multi-dose pharmacokinetic profile is complicated in mice due to altered plasma pharmacokinetic profiles following multiple intravenous and oral doses when compared to a single dose [45]. The peak plasma voriconazole concentration after 5 days of multiple doses, $2.32 \pm 1.52 \mu\text{g/mL}$ (Table 2), was significantly lower than that observed following a single dose, $7.9 \pm 0.68 \mu\text{g/mL}$ (Table 1). The peak plasma voriconazole concentration was also lower than the concentration associated with toxicity in human studies (6–7 $\mu\text{g/mL}$) and should therefore correlate with acceptable dose tolerability and side effect profiles following multiple doses [46]. However, trough plasma voriconazole concentrations had no discernable trend between day 3 and day 12 with concentrations ranging from 0.18 to 0.32 $\mu\text{g/mL}$ (Table 2). The trough plasma concentrations observed in this study were affected, in part, by the altered dosing interval, and were lower than 1 $\mu\text{g/mL}$, the trough concentration correlated with improved efficacy in humans [47]. Additionally, the influence of altered drug metabolism on plasma concentrations following multiple inhaled doses is uncertain based on this study.

Changes in voriconazole metabolism were not investigated in this current study. There is a very low prevalence of drug metabolizing enzymes in lung tissue [48,49]. Mice livers are also of insufficient size for quantitative determination of hepatic metabolic enzyme evaluation. Therefore, altered metabolism was unlikely to affect voriconazole lung pharmacokinetic parameters following multiple doses but could account for the changes in plasma voriconazole concentrations. Specifically, the single-dose pharmacokinetic profile of inhaled voriconazole suggested drug

accumulation in the lung tissue and plasma would be insignificant following multiple doses. Negligible but quantifiable drug accumulation was evidenced in lung tissue through 12 days of dosing with undetectable trough concentrations on day 5 that increased to the values of 0.19 µg/g wet lung weight on day 12 (Table 2). The peak lung voriconazole concentration on day 5 was 6.73 ± 3.64 µg/g wet lung weight was not significantly different than the observed value following a single dose (Table 1). However, peak plasma voriconazole concentrations were significantly lower following multiple doses compared to a single inhaled dose and could be influenced by altered metabolism.

Mice were selected as the pharmacokinetic model for inhaled voriconazole despite several limitations. Additionally, reports using the Aeroneb® Pro vibrating mesh nebulizer have correlated acceptable *in vitro* aerosol characteristics with low lung deposition in humans [50,51]. Published studies have demonstrated lower lung deposition of inhaled aerosols in rodents compared to humans due to allometric differences between species [52–54]. Voriconazole is also hyper-metabolized in mice and rats when administered orally and intravenously [45]. Investigators have successfully elevated voriconazole serum concentrations and improved murine survival in a model of fungal infection through the inhibition of voriconazole metabolism by grapefruit juice administration [41,55]. In the present study, no enzymatic inhibition was undertaken. Despite the limitations of low lung deposition and hyper-metabolism, pharmacokinetic profiles of voriconazole in lung tissue and plasma following single and multiple doses demonstrated high drug concentrations as well as elevated drug exposure levels.

5. Conclusions

An inhaled aqueous solution of voriconazole and sulfobutyl ether-β-cyclodextrin is capable of producing clinically relevant lung tissue and plasma concentrations. Rapid and extensive drug distribution from the lung tissue into the blood was observed leading to potential advantages over contemporary reports of inhaled antifungals. Solubilization of voriconazole by complexation with sulfobutyl ether-β-cyclodextrin potentially contributed to the observed pharmacokinetic properties. High lung tissue as well as plasma concentrations was observed following single and multiple inhaled doses. Further studies are needed to demonstrate the influence of dosing interval on voriconazole concentrations following multiple inhaled doses. However, inhaled voriconazole presents a potentially beneficial improvement in therapeutic options for the treatment of IA.

Acknowledgement

The authors thank CyDex Pharmaceuticals, Inc. for its financial support.

References

- [1] T.F. Patterson, Advances and challenges in management of invasive mycoses, *Lancet* 366 (9490) (2005) 1013–1025.
- [2] G. Chamilos et al., Invasive fungal infections in patients with hematologic malignancies in a tertiary care cancer center: an autopsy study over a 15-year period (1989–2003), *Haematologica* 91 (7) (2006) 986–989.
- [3] U. Pai et al., Invasive cavity pulmonary aspergillosis in patients with cancer: a clinicopathologic study, *Hum. Pathol.* 25 (3) (1994) 293–303.
- [4] M.D. Richardson, Changing patterns and trends in systemic fungal infections, *J. Antimicrob. Chemother.* 56 (Suppl. 1) (2005) i5–i11.
- [5] M. Cornet et al., Epidemiology of invasive aspergillosis in France: a six-year multicentric survey in the Greater Paris area, *J. Hosp. Infect.* 51 (4) (2002) 288–296.
- [6] T.J. Walsh et al., Treatment of aspergillosis: clinical practice guidelines of the Infectious Diseases Society of America, *Clin. Infect. Dis.* 46 (3) (2008) 327–360.

- [7] R. Herbrecht et al., Voriconazole versus amphotericin B for primary therapy on invasive aspergillosis, *N. Engl. J. Med.* 347 (6) (2002) 408–415.
- [8] L.J. Scott et al., Voriconazole: a review of its use in the management of invasive fungal infections, *Drugs* 67 (2) (2007) 269–298.
- [9] S. Gabardi et al., Invasive fungal infections and antifungal therapies in solid organ transplant recipients, *Transpl. Int.* 20 (12) (2007) 993–1015.
- [10] U. Theuretzbacher et al., Pharmacokinetic/pharmacodynamic profile of voriconazole, *Clin. Pharmacokin.* 45 (7) (2006) 649–663.
- [11] B. Capitano et al., Intrapulmonary penetration of voriconazole in patients receiving an oral prophylactic regimen, *Antimicrob. Agents Chemother.* 50 (5) (2006) 1878–1880.
- [12] Vfend Package Insert (2006) 47.
- [13] Z. Erjavec et al., Tolerance and efficacy of amphotericin B inhalations for prevention of invasive pulmonary aspergillosis in hematological patients, *Eur. J. Clin. Microbiol.* 16 (5) (1997) 364–368.
- [14] H.W. Boucher et al., Newer systemic antifungal agents: pharmacokinetics, safety and efficacy, *Drugs* 64 (18) (2004) 1997–2020.
- [15] J. Gavalda et al., Efficacy of nebulized liposomal amphotericin B in treatment of experimental pulmonary aspergillosis, *Antimicrob. Agents Chemother.* 49 (7) (2005) 3028–3030.
- [16] E.J. Ruijgrok et al., Aerosol delivery of amphotericin B desoxycholate (Fungizone) and liposomal amphotericin B (AmBisome): aerosol characteristics and in-vivo amphotericin B deposition in rats, *J. Pharm. Pharmacol.* 52 (6) (2000) 619–627.
- [17] E.J. Ruijgrok et al., Efficacy of aerosolized amphotericin B desoxycholate and liposomal amphotericin B in the treatment of invasive pulmonary aspergillosis in severely immunocompromised rats, *J. Antimicrob. Chemother.* 48 (1) (2001) 89–95.
- [18] C.A. Alvarez et al., Aerosolized nanostructured itraconazole as prophylaxis against invasive pulmonary aspergillosis, *J. Infect.* 55 (1) (2007) 68–74.
- [19] B.J. Hoeben et al., In vivo efficacy of aerosolized nanostructured itraconazole formulations for prevention of invasive pulmonary aspergillosis, *Antimicrob. Agents Chemother.* 50 (4) (2006) 1552–1554.
- [20] J.T. McConville et al., Targeted high lung concentrations of itraconazole using nebulized dispersions in a murine model, *Pharm. Res.* 23 (5) (2006) 901–911.
- [21] J.M. Vaughn et al., Single dose and multiple dose studies of itraconazole nanoparticles, *Eur. J. Pharm. Biopharm.* 63 (2) (2006) 95–102.
- [22] J.M. Vaughn et al., Murine airway histology and intracellular uptake of inhaled amorphous itraconazole, *Int. J. Pharm.* 338 (1–2) (2007) 219–224.
- [23] R.H. Drew et al., Comparative safety of amphotericin B lipid complex and amphotericin B desoxycholate as aerosolized antifungal prophylaxis in lung-transplant recipients, *Transplantation* 77 (2) (2004) 232–237.
- [24] I. Bekersky et al., Safety, toxicokinetics and tissue distribution of long-term intravenous liposomal amphotericin B (AmBisome): a 91-day study in rats, *Pharm. Res.* 17 (12) (2000) 1494–1502.
- [25] N. Collette et al., Tissue concentrations and bioactivity of amphotericin B in cancer patients treated with amphotericin B-desoxycholate, *Antimicrob. Agents Chemother.* 33 (3) (1989) 362–368.
- [26] K.J. Christiansen et al., Distribution and activity of amphotericin B in humans, *J. Infect. Dis.* 152 (5) (1985) 1037–1043.
- [27] T. Koizumi et al., Pharmacokinetic evaluation of amphotericin B in lung tissue: lung lymph distribution after intravenous injection and airspace distribution after aerosolization and inhalation of amphotericin B, *Antimicrob. Agents Chemother.* 42 (7) (1998) 1597–1600.
- [28] K.M. Wasan et al., Pharmacokinetics, distribution in serum lipoproteins and tissues, and renal toxicities of amphotericin B and amphotericin B lipid complex in a hypercholesterolemic rabbit model: single-dose studies, *Antimicrob. Agents Chemother.* 42 (12) (1998) 3146–3152.
- [29] P. Diot et al., Deposition of amphotericin B aerosols in pulmonary aspergilloma, *Eur. Respir. J.* 8 (8) (1995) 1263–1268.
- [30] F. Marra et al., Amphotericin B disposition after aerosol inhalation in lung transplant recipients, *Ann. Pharmacother.* 36 (1) (2002) 46–51.
- [31] W. Yang et al., High bioavailability from nebulized itraconazole nanoparticle dispersions with biocompatible stabilizers, *Int. J. Pharm.* 361 (1–2) (2008) 177–188.
- [32] USP 31 – NF 26, The United States Pharmacopeial Convention, Rockville, MD, 2008.
- [33] A. Pascual et al., Variability of voriconazole plasma levels measured by new high-performance liquid chromatography and bioassay methods, *Antimicrob. Agents Chemother.* 51 (1) (2007) 137–143.
- [34] I. Lutsar et al., Voriconazole concentrations in the cerebrospinal fluid and brain tissue of guinea pigs and immunocompromised patients, *Clin. Infect. Dis.* 37 (5) (2003) 728–732.
- [35] G. Maschmeyer et al., Invasive aspergillosis: diagnosis and management in immunocompromised patients, *Drugs* 67 (11) (2007) 1567–1601.
- [36] R.E. Lewis et al., Comparative analysis of amphotericin B lipid complex and liposomal amphotericin B kinetics of lung accumulation and fungal clearance in a murine model of acute invasive pulmonary aspergillosis, *Antimicrob. Agents Chemother.* 51 (4) (2007) 1253–1258.
- [37] S.J. Lin et al., Aspergillosis case-fatality rate: systematic review of the literature, *Clin. Infect. Dis.* 32 (3) (2001) 358–366.
- [38] M.P. Lambros et al., Disposition of aerosolized liposomal amphotericin B, *J. Pharm. Sci.* 86 (9) (1997) 1066–1069.
- [39] R. Suzuki, A.N. Freed, Hypertonic saline aerosol increases airway reactivity in the canine lung periphery, *J. Appl. Physiol.* 89 (6) (2000) 2139–2146.

- [40] A.N. Freed et al., Hyperosmotic-induced bronchoconstriction in the canine lung periphery, *J. Appl. Physiol.* 67 (6) (1989) 2571–2578.
- [41] A.M. Sugar, X.P. Liu, Effect of grapefruit juice on serum voriconazole concentrations in the mouse, *Med. Mycol.* 38 (3) (2000) 209–212.
- [42] T. Nakate et al., Improvement of pulmonary absorption of cyclopeptide FK224 in rats by co-formulating with beta-cyclodextrin, *Eur. J. Pharm. Biopharm.* 55 (2) (2003) 147–154.
- [43] K. Koushik et al., Pulmonary delivery of deslorelin: large-porous PLGA particles and HPbeta CD complexes, *Pharm. Res.* 21 (7) (2004) 1119–1126.
- [44] A. Hussain et al., Absorption enhancers in pulmonary protein delivery, *J. Control. Release* 94 (1) (2004) 15–24.
- [45] S.J. Roffey et al., The disposition of voriconazole in mouse, rat, rabbit, guinea pig, dog, and human, *Drug Metab. Dispos.* 31 (6) (2003) 731–741.
- [46] S. Husain et al., Voriconazole prophylaxis in lung transplant recipients, *Am. J. Transplant.* 6 (12) (2007) 3008–3016.
- [47] R.J.M. Brueggemann et al., Therapeutic drug monitoring of voriconazole, *Therap. Drug Monitor.* 30 (4) (2008) 403–411.
- [48] M. Nishimura et al., Tissue distribution of mRNA expression of human cytochrome P450 isoforms assessed by high-sensitivity real-time reverse transcription PCR, *Yakugaku Zasshi* 123 (5) (2003) 369–375.
- [49] J.Y. Zhang et al., Xenobiotic-metabolizing enzymes in human lung, *Curr. Drug Metab.* 7 (8) (2006) 939–948.
- [50] J.C. Dubus et al., Aerosol deposition in neonatal ventilation, *Pediatr. Res.* 58 (1) (2005) 10–14.
- [51] D. Clark et al., Targeting an inhaled erythropoietin Fc fusion protein (Epo-Fc) to the Human Large Central Airways, *Int. Soc. Aerosols Med.* (2003).
- [52] B. Asgharian et al., Empirical modeling of particle deposition in the alveolar region of the lungs: a basis for interspecies extrapolation, *Fund. Appl. Toxicol.* 27 (2) (1995) 232–238.
- [53] V. Nadihe et al., Evaluation of nose-only aerosol inhalation chamber and comparison of experimental results with mathematical simulation of aerosol deposition in mouse lungs, *J. Pharm. Sci.* 92 (5) (2003) 1066–1076.
- [54] American Institute of Ultrasound in Medicine, Section 3 – selected biological properties of tissues: potential determinants of susceptibility to ultrasound-induced bioeffects, *J. Ultrasound. Med.* 19(2) (2000) 58–96.
- [55] J.R. Graybill et al., Improving the mouse model for studying the efficacy of voriconazole, *J. Antimicrob. Chemother.* 51 (6) (2003) 1373–1376.